

# Chapter 2

## Fragility Curves

### 2.1 Historical Background

Many previous studies, such as those of Kiremidjian (1992), Kunitani and Takada (2004), Akkar et al. (2005), Frankie et al. (2012), Bakhshi and Asadi (2013), Modica and Stafford (2014), Silva et al. (2014), Pragalath et al. (2015), Cutfield et al. (2016), and Joy et al. (2016), present a brief historical background of fragility curve. In these book, fragility curves are defined as the probability of reaching or exceeding a specific damage state under earthquake excitation.

The general equation to develop fragility or conditional probability is expressed by Billah and Alam (2014)

$$\text{Fragility} = P[\text{LS}|\text{IM} = y], \quad (2.1)$$

where,

LS is the limit state or damage state (DS),

IM is the intensity measure (ground motion), and

$Y$  is the realized condition of ground motion IM.

Various equations were derived from previous research (Table 2.1). However, all the equations are based on Eq. (2.1), which is a general equation for generating a fragility curve.

Although most of these studies used different equations to generate their versions of the seismic fragility curves (Table 2.1), most researchers such as Yamaguchi and Yamazaki (2000), Kirçil and Polat (2006), and Ibrahim and El-Shami (2011) used Eq. (2.2) in their studies. This equation is the simplest one in the group. Yamaguchi and Yamazaki (2000) tested Eq. (2.2) for different types of structures and found it to be suitable for use in all structural types. This equation is given below:

**Table 2.1** Equations used to develop the fragility curve

| Authors                           | Equation  | Parameters  | Structure type   |
|-----------------------------------|---|---|--|
| Hwang and Jaw<br>(1990)           | $P_f = \Phi \left[ \frac{-\ln \left( \frac{\mu_R}{\mu_E} \right)}{(\beta_R^2 + \beta_E^2)^{1/2}} \right]$ | $P_f$ = probability<br>$\Phi[\cdot]$ = standardize normal distribution<br>$\mu_R$ = median capacity based on engineering judgment<br>$\beta_R$ = standard deviation based on engineering judgment<br>$\mu_E$ = median from sample<br>$\beta_E$ = standard deviation from sample | Shear wall   |
| Seya et al. (1993)                | $P_f = P_r(R < S) = \int_0^\infty [1 - F_S(r)] f_R(r) dr$   | $P_f$ = probability conditional limit state<br>$R$ = structural capacity<br>$S$ = structural response<br>$F_S(\cdot)$ = cumulative probability distribution of $S$<br>$f_R$ = probability density function of $R$   | MRSF   |
| Singhal and Kiremidjian<br>(1996) | $P_{D MMI}[d MMI] = \int_{S_a} P_{D S_a}[d S_a] f_{S_a MMI}[S_a MMI] dS_a$                                | $P_{D MMI}[d MMI]$ = probability reaching or exceed at specified MMI<br>$P_{D S_a}[d S_a]$ = probability reaching or exceed at specified spectral acceleration<br>$f_{S_a MMI}[S_a MMI]$ = conditional probability density function of spectral acceleration at specified MMI   | MRCF   |
| Yamaguchi and Yamazaki (2000)     | $P(x) = \Phi \left( \frac{\ln x - \lambda}{\varsigma} \right)$  | $\Phi[\cdot]$ = standardize normal distribution<br>$\lambda$ = mean of $\ln x$<br>$\varsigma$ = standard deviation of $\ln x$   | i. Wood-frame<br>ii. Wooden-prefabricated<br>iii. RC<br>iv. Steel-frame<br>v. Light-gauge steel-prefabricated<br>(continued) |

Table 2.1 (continued)

| Authors                        | Equation  | Parameters  | Structure type          |
|--------------------------------|---|---|-------------------------|
| Rosowsky and Ellingwood (2002) | $FR(x) = \Phi \left[ \ln \frac{(\lambda/m_R)}{\xi_R} \right]$   | $\Phi[\cdot]$ = standardize normal distribution<br>$m_R$ = median capacity<br>$x$ = demand<br>$\xi_R$ = logarithmic standard deviation  | Light wood-frame        |
| Kiril and Polat (2006)        | $P(\leq D) = \Phi \left( \frac{\ln x - \hat{\lambda}}{\xi} \right)$   | $\Phi[\cdot]$ = standardize normal distribution<br>$X$ = lognormal distributed ground motion index (e.g. $S_w$ , $S_a$ , PGA)<br>$\hat{\lambda}$ = mean<br>$\xi$ = standard deviation   | RC residential building |
| Lupoi et al. (2006)            | $P_f(y_1) = \Pr \left\{ \bigcup_{j=1}^{n_C} I \in I_{C_j} \cap C_i(x, \varepsilon_{C_i}) \leq D_i(x y_1) \right\}$  | $n_C$ = number of cut-sets<br>$I_{C_j}$ = set of the indices of modes belonging to the $j$ th cut-set   | 3D RC building          |
| Luco et al. (2011)             | For undamaged, $\Pr[IM > a] = 1 - \Phi \left[ \frac{\ln a - \ln m_{IM}}{\sigma_{\ln IM}} \right]$<br>For damaged (post-mainshock),<br>$\Pr[DS > i] = \int_0^\infty \Pr[DS > i   IM = a] \left  \frac{d \Pr[IM > a]}{da} \right  da$ | $\Pr[IM > a]$ = fragility for pre-mainshock (undamaged)<br>$m_{IM}$ = median of the IM at each location<br>$\sigma_{\ln IM}$ = logarithmic standard deviation<br>$\Pr[DS = i]$ = post-mainshock damage state probabilities              | MRCF                    |
| Ibrahim and El-Shami (2011)    | $P[D/PGA] = \Phi \left( \frac{\ln(PGA) - \mu}{\sigma} \right)$  | $\Phi[\cdot]$ = standardize normal cumulative distribution<br>$\mu$ = mean of natural logarithm<br>$\sigma$ = standard deviation of natural logarithm   | MRCF                    |
| R  veill  re et al. (2012)     | $P(DS \geq k   DS_0 = i, IM) = \phi \left( \frac{\ln a - \ln \mu_{i,k}}{h_{i,k}} \right)$   | $\phi$ = cumulative distributive function of standard normal distribution<br>$\mu_{i,k}$ = median of fragility curve from $DS = i$ to $DS \geq k$<br>$\beta_{i,k}$ = standard deviation of fragility curve from $DS = i$ to $DS \geq k$ | MRCF                    |

(continued)

Table 2.1 (continued)

| Authors               | Equation   | Parameters   | Structure type             |
|-----------------------|--|--|----------------------------|
| Jeon et al. (2012)    | $P[D_{as} > C IM_{as}] = \Phi \left[ \frac{\ln(S_d/S_c)}{\sqrt{\beta_{d IM_{as}}^2 + \beta_c^2 + \beta_m^2}} \right]$  | $D_{as}$ = seismic demand (aftershock)<br>$C$ = structural capacity<br>$S_d$ = median of demand<br>$\beta_{d IM}$ = dispersion of demand<br>$S_c$ = median of capacity<br>$\beta_c$ = dispersion of capacity<br>$\beta_m$ = modeling uncertainty ( $\beta_m = 0.2$ )     | MRCF                       |
| Frankie et al. (2012) | $P(\text{Exceedance}_i IM) = \Phi \left[ \frac{1}{\beta_{tot,i}} \ln \left( \frac{IM}{LS_i} \right) \right]$   | $\Phi[\cdot]$ = standardize normal cumulative distribution<br>$(\beta_{tot})_i$ = log SD represent total uncertainty<br>$LS_i$ = threshold value for $i$ th limit state  | Unreinforced-masonry (URM) |
| Polese et al. (2013)  | $P[\text{col} a_g] = \Phi \left[ \frac{1}{\beta} \cdot \ln \left( \frac{a_g}{a_g} \right) \right] = \Phi \left[ \frac{1}{\beta} \cdot \ln \left( \frac{a_g}{REC_{ag}} \right) \right]$ | $P[\text{col} a_g]$ = probability of attaining collapse state given peak ground acceleration<br>$a_g$ = peak ground acceleration<br>$\Phi[\cdot]$ = standardize normal cumulative distribution<br>$\beta$ = global value of dispersion<br>$REC_{ag}$ = residual capacity | MRCF                       |
| Sudret et al. (2013)  | $\text{Frag}(PGA) = 1 - \Phi \left( \frac{\ln \delta_0 - [\Lambda \ln(PGA) + B]}{\zeta} \right)$   | $PGA$ = peak ground acceleration<br>$\Phi[\cdot]$ = standardize normal cumulative distribution<br>$\delta_0$ = admissible threshold<br>$\Lambda, B$ = mean of linear regression in a log-log plot<br>$\zeta$ = standard deviation  | MRSF                       |

(continued)

Table 2.1 (continued)

| Authors                 | Equation  | Parameters   | Structure type                          |
|-------------------------|---|--|---|
| Negulescu et al. (2014) | $P_f(ds \geq ds_i   S) = \Phi \left[ \frac{1}{\beta_{tot}} \cdot \ln \left( \frac{IM}{IM_m} \right) \right]$          | $P_f(\cdot)$ = probability of exceeding a particular damage state, $ds$ , for a given intensity level (PGA)<br>$\Phi$ = standard cumulative probability function<br>$IM_{mi}$ = median threshold value of earthquake intensity measure<br>$\beta_{tot}$ = lognormal standard deviation | Masonry building reinforced by tie rods |
| Barbat et al. (2014)    | $P[i/sd] = \Phi \left[ \frac{1}{\beta_{ds_i}} \cdot Ln \left( \frac{sd}{sd_{ds_i}} \right) \right]$                   | $sd$ = spectral displacement<br>$sd_{ds_i}$ = mean value of lognormal distribution which corresponds to damage state threshold<br>$\beta_{ds_i}$ = standard deviation of natural logarithm of spectral displacement of $ds$  | MRCF                                    |
| Lee et al. (2014)       | $P[C < D   SI = x] = 1 - \Phi \left[ \frac{\ln(\hat{C}/D)}{\sqrt{\beta_{DSI}^2 + \beta_c^2 + \beta_m^2}} \right]$     | $\Phi[\cdot]$ = standard normal probability integral<br>$\hat{C}$ = median structural capacity<br>$\hat{D}$ = median structural demand<br>$\beta_{DSI}$ = uncertainty in $D$<br>$\beta_c$ = uncertainty in $C$<br>$\beta_m$ = modeling uncertainty                                     | RC building in Y-shaped and box-shaped  |
| Farsangi et al. (2014)  | $P_f = P \left\{ \bigcup_{i=1}^n \left[ \max_{h_i} \frac{u_i}{h_i} \geq LS   IM \right] \right\}_r$ and $0 < t < t_d$ | $t_d$ = duration of the ground motion<br>$i$ = storey level<br>$n$ = number of storey<br>$u_i$ = storey drift<br>$h_i$ = storey height   | MRSF                                    |
| Hancilar et al. (2014)  | $P_f(\text{Damage} \geq DS_i   IM) = \Phi[(1/\beta) \ln(IM/\mu)]$   | $\Phi$ = standard cumulative probability function<br>$\beta$ = log-standard deviation of IM<br>$\mu$ = mean of IM  | MRCF with shear wall                    |
| (continued)             |   |  |   |

Table 2.1 (continued)

| Authors  | Equation   | Parameters  | Structure type                            |
|--|--|---|---|
| Vona (2014)                                      | $P[d_{SI} I_H] = \Phi\left[\frac{1}{\beta_{ds_i}} \cdot \ln\left(\frac{I_H}{\mu_{ds_i}}\right)\right]$                             | $\Phi$ = standard normal cumulative probability function<br>$\mu_{ds}$ = median value of Housner intensity of damage state<br>$\beta_{ds_i}$ = standard deviation of lognormal of Housner Intensity   | MRCF                                      |
| Banihashemi et al. (2015)                        | $P(D > d_i   I_m) = 1 - P(D \leq d_i   I_m) = 1 - \Phi\left(\frac{\ln\left(\frac{SD_i}{\sqrt{SD_{im}}}\right)}{\beta_{im}}\right)$ | $\sqrt{SD_{im}}$ = medians of ISD distribution<br>$\beta_{im}$ = deviation lognormal distribution of ISD in each im<br>$ISD_i$ = threshold of different damage state  | Steel concentrically braced frames (SCBF) |
| Wijayanti et al. (2016) and McCrum et al. (2016) | $P[ds S_d] = \Phi\left[\frac{1}{\beta_{ds}} \ln\left(\frac{S_d}{S_{d,ds}}\right)\right]$   | $S_d$ = spectral displacement<br>$S_{d,ds}$ = median value of spectral displacement at which the building reaches the threshold of the damage state, ds<br>$\beta_{ds}$ = standard deviation of the natural logarithm of spectral displacement of damage state, ds<br>$\Phi$ = standard normal cumulative distribution function | MRCF                                      |
| Akhavan et al. (2016)                            | $F_d(x) = P[D \geq d X = x]; d \in \{1, 2, \dots, N_D\} = \Phi\left(\frac{\ln(x/\theta_d)}{\beta_d}\right)$                        | $D$ = uncertain damage state of particular component<br>$d$ = particular value of D<br>$X$ = uncertain excitation<br>$x$ = particular value of X<br>$\theta_d$ = median capacity<br>$\beta_d$ = standard deviation of natural logarithm of capacity   | MRSF                                      |

(continued)

Table 2.1 (continued)

| Authors                     | Equation   | Parameters  | Structure type   |
|-----------------------------|--|---|--|
| Pejovic and Jankovic (2016) | $P[DS_i = IDR > IDR^{DS_i}/IM] = \Phi\left(\frac{IM - \mu}{\sigma}\right)$ | $\Phi$ = standard normal cumulative distribution function<br>$\mu$ = mean value<br>$\sigma$ = standard deviation<br>$IM$ = intensity measure<br>$IDR$ = inter-storey drifts | MRCF (high-rise building with core wall structural system) |

$$P(x) = \Phi\left(\frac{\ln X - \lambda}{\varsigma}\right) \quad (2.2)$$

where,

- $\Phi[\cdot]$  is the standardize normal distribution,
- $\lambda$  is the mean of  $\ln x$ , and
- $\varsigma$  is the standard deviation of  $\ln x$ .

The fragility curves are established to provide a prediction of potential damage during an earthquake. These curves represent the seismic risk assessment and are used as an indicator to identify the physical damage in the strongest mainshock. Apart from the mainshock, probability aftershock must also be investigated to decide whether or when to permit re-occupancy of a building. The fragility function is also directly used to reduce damage cost and loss of life during a seismic event. Therefore, fragility curves can be used as a decision-making tool for both pre- and post-earthquake situations. Moreover, these curves may help develop future local code provisions.

Two main components in the probabilistic seismic risk assessment have been identified. These components include information about ground motion hazard on the location of structure and fragility knowledge with respect to the intensity of the ground motion. Polese et al. (2014) stated four important factors available for a large database, which include the number of storeys, age of construction, regularity (in plan, elevation, and in-fill), and position of building in the block. Silva et al. (2014) proposed vulnerability curves using the HAZUS tool (HAZUS 1999) for risk assessment. The curves were created specifically for buildings in the US.

## 2.2 Structural Types

Fragility curves were discussed based on three types of structures, namely, steel, reinforced concrete, and timber. Most studies covered steel and reinforced concrete structures. However, less research has been conducted on timber structure. Many studies developed fragility curves for infrastructures, including those of Shinozuka et al. (2000), Alessandri et al. (2011), Billah and Alam (2014), and Siqueira et al. (2014). However, the fragility curves for buildings are categorized into three types. These types are low-, mid-, and high-rise buildings based on the number of storeys (Table 2.2).

The important factors of vulnerability, which are also available for large databases, include a number of storeys, age of construction, regularity in plan and elevation, infill regularity, and building position in the block (Polese et al. 2014). Thus, classifying buildings is one of the significant factors that must be considered in developing fragility curve. Differences in materials, height, and number of bays also result in different shapes of vulnerability curves. Researchers from different



**Table 2.2** Classification of Building by Number of Storeys

| Authors  | Building Classification |          |           |
|--|-------------------------|----------|-----------|
|  | Low-rise                | Mid-rise | High-rise |
|  | Number of storeys       |          |           |
| Singhal and Kiremidjian (1996), Akkar et al. (2005), Uma et al. (2011) | 1–3                     | 4–7      | 8 and up  |
| Modica and Stafford (2014), Silva et al. (2014a)                       | 1–3                     | 4–6      | 7 and up  |
| Hancilar et al. (2014)   | 1–4                     | 5–8      | 9 and up  |

countries have developed their respective versions of the curve. Table 2.3 shows the synopsis of fragility analysis performed by several researchers.

2.3 Earthquake Records

Ground motion records play the main role in establishing fragility curves. Selecting an appropriate ground motion and scaling the ground motions are very important in generating this curve. If the ground motion is randomly scaled up to a specific spectral acceleration,  $S_a$ , at a period,  $T$ , over conservative structural response may occur (Baker et al. 2014).

A few parameters must be considered in selecting ground motion, including event magnitude, peak ground acceleration (PGA), distance between epicenter/ source and affected area, and soil type (Nazri and Alexander 2012). In addition, ground motion characteristics must be considered to obtain accurate prediction and to minimize the dispersion of the analytical behavior of buildings. Ground motion characteristics that must be considered include, ground motion intensity, spectral shape, duration, frequency content, near-fault, amplitude, and number of cycles (Ibrahim and El-Shami 2011; Ruiz-García and Negrete-Manriquez 2011; Song et al. 2014).

The selected ground motion must come from previously recorded earthquake events. Ground motion can be selected from certain websites, such as Pacific Earthquake Engineering Research (PEER) NGA database website, Consortium of Organization for Strong Motion Observation System, or K-NET. Silva et al. (2014) list other websites where ground motion records can be obtained, including the European Strong Motion database, the French Accelerometric Network, and the Swiss Earthquake Database.

The suitable number of ground motions depends on the application and structural response prediction. Two types of ground motions are considered as fore-shocks: near-field site and far-field site. Researchers discuss a few important factors in selecting ground motion. For far-field site, the important factors include spectral shape over the period range of interest, magnitude, site-to-source distance, and hazard curve at a period,  $T$ . Meanwhile, for near-field site, the factors to be

**Table 2.3** Summary from Prior Studied

| Authors                        | Highlight   | Type of structure       | Number of storeys | Number of bays |
|--------------------------------|---|-------------------------|-------------------|----------------|
| Hwang and Jaw (1990)           | Show a simplified analytical method to develop fragility curve and give an overview about fragility background  | Shear wall              | 5                 | –              |
| Seya et al. (1993)             | Generate fragility curve for steel frame  | MRSF                    | 5                 | 3              |
| Holmes (1996)                  | Show a general step and provide information about fragility curve   | –                       | –                 | –              |
| Singhal and Kiremidjian (1996) | Use nonlinear history analysis to generate fragility curve  | MRCF                    | 2, 5, 12          | 5              |
| Kircher et al. (1997)          | Describe general information about damage, methods to estimate probability on both structural and nonstructural parts developed for the FEMA/NIBS   | –                       | –                 | –              |
| Yamaguchi and Yamazaki (2000)  | Five different types of materials, namely, wood-frame, wooden-fabricated, reinforced concrete (RC), steel-frame, and light-gauge steel-prefabricated, were tested to develop fragility curve based on Kobe earthquake in 1995           | Frame                   | –                 | –              |
| Lee and Rosowsky (2006)        | Develop an appropriate percentage of design snow loads for fragility seismic assessment   | Shear wall (wood-frame) | 1 and 2           | 1              |
| Ibrahim and El-Shami (2011)    | Discuss the method to develop fragility curve for low- and mid-rise concrete frame  | MRCF                    | 3 and 8           | 3              |
| Uma et al. (2011)              | Present the different parameters in the structural model and their impact on vulnerability risk assessment for mainshock and aftershock records. Typical building model in New Zealand and the United States was generic for this study | MRCF                    | 5                 | –              |

(continued)

**Table 2.3** (continued)

| Authors                  | Highlight   | Type of structure | Number of storeys | Number of bays |
|--------------------------|---|-------------------|-------------------|----------------|
| Jeon et al. (2012)       | Evaluate the seismic cumulative damage potential of non-ductile reinforced concrete and their performance and increase the vulnerability after multiple earthquakes   | MRCF              | 3                 | 3              |
| Sudret et al. (2013)     | Generate seismic vulnerability curve by using polynomial chaos expansions for steel frame   | MRSF              | 3                 | 3              |
| Goda and Salami (2014)   | Study the impact of aftershock on seismic vulnerability of conventional timber frame houses by using a set of real mainshock and aftershock earthquake records  | Timber frame      | 2                 | 1              |
| Kumar et al. (2014)      | Propose a simple methodology to assess the probabilistic seismic damage of RC buildings by using nonlinear pushover analysis  | MRCF              | 4                 | 1              |
| Farsangi et al. (2014)   | Develop fragility curve and estimate mean annual seismic loss for MRSF in the Middle East area  | MRSF              | 2                 | 2              |
| Ebrahimian et al. (2014) | Develop vulnerability curve and investigate adaptive aftershock risk assessment in terms of daily limit state first-excursion probabilities. In this study, cloud analysis was implemented to develop the fragility curve | MRCF              | 3                 | 2              |
| Jalayer et al. (2014)    | Introduce Bayesian cloud analysis in the fragility curve. Then, this analysis was compared with IDA analysis  | MRCF              | 4                 | 4              |
| Shin et al. (2014)       | Propose a methodology to assess the effectiveness of retrofitting with buckling resistance brace  | MRCF              | 5                 | 2              |
| Silva et al. (2014a)     | Develop fragility curve for Portuguese RC building  | MRCF              | –                 | 3              |

(continued)

**Table 2.3** (continued)

| Authors                   | Highlight  | Type of structure                         | Number of storeys | Number of bays |
|---------------------------|--|---|-------------------|----------------|
| Barbat et al. (2014)      | Develop fragility curve and investigate the seismic damage in RC in terms of probability by using Monte Carlo  | MRCF                                      | 8                 | 6              |
| Silva et al. (2014b)      | Estimate the nonlinear response of building by using static and dynamic procedure and investigate the effectiveness of the capacity, fragility, and risk   | MRCF                                      | 4                 | 3              |
| Hancilar et al. (2014)    | Assess and develop a probabilistic curve for a public school in Istanbul   | MRCF                                      | 4                 | 11             |
| Li et al. (2014)          | Study the collapse probability mainshock damage to steel building in aftershock  | MRSF                                      | 4                 | 4              |
| Aiswarya and Mohan (2014) | Develop fragility curve for flat slab structure and evaluate the seismic vulnerability. Then, determine a method to improve the seismic performance. Unretrofitted and retrofitted structure fragility curves were compared for an office located in Mid-American region | Reinforced concrete flat slab building    | 5                 | 4              |
| Pragalath et al. (2015)   | Propose two techniques to develop seismic fragility curve based on time history analysis and IDA. Both methods have different assumptions and methodologies  | MRCF                                      | 4                 | 4              |
| Banihashemi et al. (2015) | A newly developed performance-based plastic design (PBD) methodology was applied to steel special concentric braced frames. Reliability-based assessment based on FEMA 351 indicated that PBD frames have much higher  | Steel concentrically braced frames (SCBF) | 6, 9              | 1              |

(continued)

**Table 2.3** (continued)

| Authors                 | Highlight  | Type of structure | Number of storeys | Number of bays |
|-------------------------|--|-------------------|-------------------|----------------|
|                         | confidence levels against global collapse than those of corresponding SCBFs designed by current seismic codes and the results are proved by the seismic fragility curves of model frames   |                   |                   |                |
| Wijayanti et al. (2016) | Seismic vulnerability assessment for Indonesian reinforced concrete frame building with steel truss roof by using fragility curve  | MRCF              | 4                 | —              |
| Akhavan et al. (2016)   | The seismic response of 2-D MRSF buildings incorporating soft storey is evaluated. The fragility curves for different placement of soft storey in the first, middle, and top floor for 4, 8 and 16-storey buildings are developed and compared   | MRSF              | 4, 8, 16          | 3              |
| Lin et al. (2017)       | Seismic and progressive collapse designs for RC frames are performed independently according to the corresponding design codes. Fragility curves are used to assess the seismic and progressive collapse resistance  | MRCF              | 6                 | 4              |
| McCrum et al. (2016)    | Demonstrates the development of fragility curves at different damage states using a detailed mechanical model of an MRCF structure typical of Southern Europe. The mechanical model consists of a complex 3-DFEM of the MRCF structure and is used to define the damage states through pushover analysis | MRCF              | 3                 | 1              |

(continued)

**Table 2.3** (continued)

| Authors                     | Highlight  | Type of structure  | Number of storeys | Number of bays |
|-----------------------------|--|--|-------------------|----------------|
| Pejovic and Jankovic (2016) | Seismic fragility assessment of RC high-rise buildings for seismic excitation, typical for Southern Euro-Mediterranean zone. 20-, 30-, and 40-storey RC high-rise buildings with core wall structural system were chosen. Since no probabilistic fragility curves exist for this class of buildings and for this seismic zone, this work partially fills the void in Southern Euro-Mediterranean seismic risk assessment | MRCF (high-rise building with core wall structural system) | 20, 30, 40        | –              |

considered include spectral shape and the possible presence of velocity pulses. Table 2.4 presents an overview of recommendations for selecting and scaling ground motion (Haselton et al. 2012).

Apart from obtaining data from the aforementioned databases, ground motion records can also be generated based on the equation. For example, Sudret et al. (2014) generated ground motion records from several equations. The procedure to simulate synthetic ground motion is briefly explained because stimulating synthetic ground motion usually takes too long. In their study, they concluded there are three temporal parameters, three spectral parameters, and a standard Gaussian random vector of size that must be considered to generate a seismic model. Compared with synthetic ground motion, real accelerograms are more widely used as ground motion records and then scaled to cover the range of ground motion level that might occur (Ay and Akkar 2014).

Reasenber and John (2005) reported that earthquakes occur in clusters, that is, when one earthquake strikes, another earthquake will occur in the nearby locations. According to Uhrhammer (1986), events that only occur in a zone approximately parallel to the fault rupture or surround the main events are considered foreshocks or aftershocks. In an earthquake event, the magnitude can be classified into three terms, namely, foreshock, mainshock, and aftershock. The largest magnitude is called mainshock, whereas the earthquakes that occur before and after the mainshock are called foreshock and aftershock, respectively. However, mainshocks are often redefined as foreshock if a subsequent earthquake in a cluster has a larger magnitude.

**Table 2.4** Recommendations for ground motions selecting and scaling modified from Haselton et al. (2012)

| Steps for response history analysis                      | Design/assessment method   |   |  |  |
|--|--|---|--|--|
|  | ASCE7-05   | ASCE-10   | LATBSDG  | PEER TBI   |
| Ground motion selection                                  | —  | —   | —  | —  |
| Number of motions  | $\geq 7$ (or 3) pairs  |   | $\geq 7$ pairs   |  |
| Types of motion  | Recorded and/or simulated  |   | Record or simulated (ref to ASCE7-05)                                | Recorded and/or simulated  |
| Other  | None   |   | Appropriate num. of motion with directivity effects                  | Directivity if needed  |
| Scaling/modification of motions to match target spectrum | —  | —   | —  | —  |
| General approach   | Scaling (spectral matching not mentioned)                        |   | Scaling or spectral matching   |  |
| Specific instructions for far-field sites                | SRSS is above target $1.17 \times$ target spectrum               | SRSS is above target spectrum                       | SRSS is above target $1.17 \times$ target spectrum (ref to ASCE7-05) | Match records to the target spectrum                             |
| Specific instructions for near-field sites               | None   | Average of FN is above target                       | None (ref to ASCE7-05)   | None   |
| Period range for matching                                | 0.2–1.5 T  |   | 0.2–1.5 T (ref to ASCE7-05)  | Not specified  |
| Application of ground motions to structural model        | —  | —   | —  | —  |
| Far-field sites  | Apply only horizontal motions together; no rules for orientation |   | Orient motions randomly; no need for multiple orientations of GMs    | Apply along principle directions if directivity effects dominate |
| Near-field sites   | No rules for orientation   | Apply in FN/FP direction if site $>5$ km from fault | Apply in FN and FP directions  | Apply in FN and FP directions if directivity effects dominate    |

SRSS—Square-Root-Sum-of Squares Spectrum (Ground motion scaling ground motion method)

FN—Fault Normal

FP—Fault Parallel

Most prior research used mainshock records as inputs in their seismic risk assessment. For example, Farsangi et al. (2014) evaluated the seismic vulnerability of moment-resisting steel frame (MRSF) using mainshock ground motion records. They explicitly explained the whole process starting from selecting ground motion records from the PEER website. Seven sets of ground motions were used and the basic characteristics of earthquakes, such as strikes and frequencies, were considered in the selection. Then, the records were scaled to the elastic response spectrum with 5% damping.

Wells and Coppersmith (1994) explained that aftershocks can occur within a few hours to a few days after the mainshock. The fault produces most of the aftershocks when the stress on the mainshock fault changes drastically during the mainshock. These earthquakes can be regarded as aftershocks if they are located within a characteristic distance from the mainshock. This distance usually takes one or two times the length of the fault rupture associated with the mainshock.

In a recent study, aftershock records have been considered in developing the fragility curve. Such aftershock has big potential to induce massive damages and losses. Several aftershock events have been recorded, such as the Chi-Chi earthquake in Taiwan. During this time, a gas station survived the mainshock and then collapsed during the aftershock. Therefore, aftershock events must also be considered in seismic risk assessment.

The methods for selecting and scaling ground motions have been investigated by several researchers (Haselton et al. 2012; Ay and Akkar 2014; Wang and Rosowsky 2014). Haselton et al. (2012) highlighted the best method for selecting and scaling ground motions. They reported that these tasks depend on three types of assessments, namely, intensity-, scenario-, and risk-based (time-based) assessments in ATC-58-1. Of these, the most commonly used is the intensity-based assessment. For selecting and scaling ground motions, proper methods are based on structural response parameter(s) of interest, and either record-to-record variability in structural response or maximum response (collapse response) must be predicted.

Wang and Rosowsky (2014) introduced three new approaches for scaling ground motions. The first approach involves selecting ground motion from the real historic seismic records. The second approach is initially selecting ground motion from the real historic seismic, and then modifying this to satisfy the given site using an amplitude scaling method or spectrum matching method. The third approach involves initially selecting ground motion from seismological model with some information and then generating synthetic ground motions.

Meanwhile, two alternative procedures have been explicitly discussed in the paper of Ay and Akkar (2014). The first proposed procedure is based on the conditional mean spectrum. The second method is based on empirical elastic-to-inelastic conversion factors. In this method, the target inelastic spectral coordinates are initially estimated, and then, the records are scaled to the estimated inelastic target level. In the study of Barbat et al. (2014), 20 acceleration records were selected. Then, these records were scaled to different levels of the peak ground acceleration. Figure 2.1 shows the mean spectrum and spectrum of Eurocode 8 corresponding to the 20 selected ground motions.



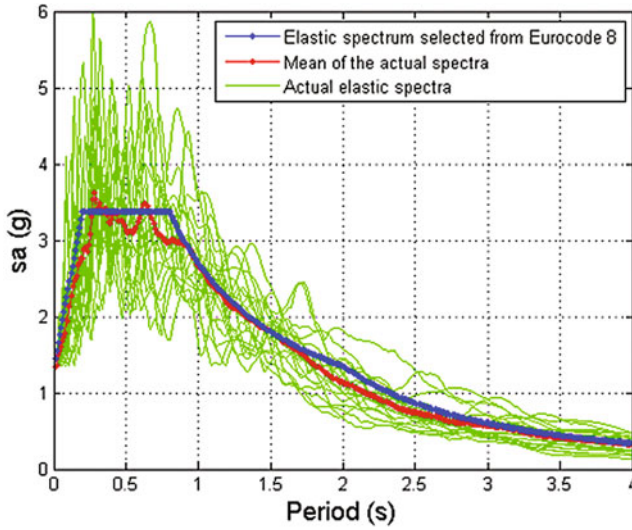


**Fig. 2.1** Mean spectrum of selected earthquake events scaled to the spectrum of Eurocode 8 (Barbat et al. 2014)

## 2.4 Simulation Methods

To develop the fragility curves using the analytical method, a few popular simulation methods need to be applied. The assessment can be categorized into two main groups, namely, NSA and NDA. Some researchers use NSA (Mosalam et al. 1997; Frankie et al. 2012; Polese et al. 2013; Vargas et al. 2013; Garcia 2014; Kumar et al. 2014; Lee et al. 2014; Lee and Moon 2014), nonlinear time history analysis (NTHA) (Aiswarya and Mohan 2014; Farsangi et al. 2014; Wang and Rosowsky 2014), and incremental dynamic analysis (IDA) (Luco et al. 2011; Ryu et al. 2011; Uma et al. 2011; Bakhshi and Asadi 2013; Charalambos et al. 2014; Raghunandan et al. 2014; Sudret et al. 2014). The next sections will present a review of different simulation methods employed to develop fragility curve. Some software are available to perform this analysis. Table 2.5 shows some of such software used by researchers.

### 2.4.1 Nonlinear Static Analysis

Nonlinear static analysis or pushover analysis (POA) is one of the methods used to develop fragility seismic curves. Polese et al. (2013) initially evaluated the appropriateness of POA in damage analysis, from which they developed the

**Table 2.5** Available software used by researchers

| Authors   | Structural type                           | Software                |
|---|---|-------------------------|
| Seya et al. (1993)  | MRSF                                      | DRAIN-2D                |
| Singhal and Kiremidjian (1996)  | MRCF                                      | DRAIN-2DX               |
| Akkar et al. (2005), Hancilar et al. (2014)   | MRCF                                      | SAP2000                 |
| Kirçil and Polat (2006)   | RC residential building (3D)              | IDARC                   |
| Lee and Rosowsky (2006)   | Wood-frame (shear wall)                   | SAW and CASHEW          |
| Lupoi et al. (2006), Ryu et al. (2011), Uma et al. (2011), Jeon et al. (2012), Réveillère et al. (2012), Shome et al. (2014), Silva et al. (2014), Hancilar et al. (2014) | MRCF (2D and 3D)                          | OpenSees                |
| Ibrahim and El-Shami (2011)   | MRCF                                      | SeismoStruct            |
| Ruiz-García and Negrete-Manriquez (2011)  | MRSF                                      | Ruaumoko                |
| Bakhshi and Asadi (2013)  | MRSF                                      | IDARCV7.0               |
| Sudret et al. (2013), Li et al. (2014), Farsangi et al. (2014)  | MRSF                                      | OpenSees                |
| Negulescu et al. (2014)   | Masonry building reinforced by tie-rods   | TREMURI                 |
| Goda and Salami (2014), Shome et al. (2014)   | Wood-frame                                | SAWS for wood structure |
| Garcia (2014)   | MRSF                                      | SAP2000                 |
| Banihashemi et al. (2015)   | Steel concentrically braced frames (SCBF) | OpenSees                |
| Wijayanti et al. (2016)   | MRCF                                      | HAZUS                   |
| Akhavan et al. (2016)   | MRSF                                      | HAZUS-MH                |
| McCrum et al. (2016)  | MRCF                                      | ABAQUS                  |
| Pejovic and Jankovic (2016)   | MRCF                                      | PERFORM-3D              |

fragility curve. They conducted the analysis of intact structures and damaged buildings, resulting in a capacity curve. Moreover, Kumar et al. (2014) mentioned that capacity curves can represent mean or mean plus/minus with one/two/three times the standard deviation of capacity curves. From these capacity curves, the results can be compared with those of the Performance-Based Seismic Design (PBSD) in generating fragility curve.

### 2.4.2 Nonlinear Dynamic Analysis

It is important to choose a nonlinear analysis tool while considering its limitation. Such a tool can provide an accurate investigation and stable NTHA of the structure

(Farsangi et al. 2014). The NDA or NTHA method considers geometric nonlinearity and material inelasticity in predicting the displacement behavior and collapse load. In addition, this method requires a ground motion. A suitable set of ground motions is needed to ensure the accuracy of the fragility curves. However, the suitability of the set of ground motion is a significant issue (Billah and Alam 2014).

Vona (2014) investigated fragility curves based on different methods of analysis, namely, POA and NDA. According to this study, it has been shown that NDA is the most accurate method for investigating the moment resisting concrete frames (MRCF) performance. This method can consider the real characteristics as inputs, from which it can evaluate structural response.

In addition, Silva et al. (2014) reported that NDA applies acceleration time history analysis, which then leads to accurate results. However, they found that NDA is time-consuming. Thus, they introduced several methods, such as capacity spectrum method, displacement coefficient method (DCM) and N2 method, as alternatives. In conclusion, they suggested use of NSA as a valid alternative for obtaining results rapidly and accurately.

Billah and Alam (2014) argued that NTHA requires a large number of ground motions, making the computational analyses expensive. Thus, they introduced IDA to replace NTHA. They mentioned that Luco and Cornell (1998) first developed this method, which used to be a part of NTHA (both are found to be similar). However, ground motion in IDA is scaled in increments, thereby, resulting in a different performance depending on the intensity level.

The aforementioned assumption is supported by Colapietro et al. (2014), who argued that IDA is an extension method of NTHA or NDA. This method properly estimates the performance of structure under seismic load through certain sets of ground motion records and scales the ground motion records to obtain the response curve. Upon comparing the results of IDA and POA methods, they concluded that POA shows good correlation with IDA. However, the POA is more conservative than the latter, especially in predicting higher mode effects in the post-elastic range, which considers irregular buildings with limited capabilities of fixed load distributions. IDA can be used to investigate complexities and extreme irregularities of analyzed buildings. Given that the reliability of an analysis is related to the level of knowledge, the authors suggest that destructive and non-destructive tests should be performed to obtain more realistic estimations of seismic variability.

Ryu et al. (2011) performed IDA analysis to develop fragility curves using a typical New Zealand 5-storey MRCF. This paper shows the process application of IDA. The first step is choosing the mainshock and aftershock ground motion records. In this study, 30 sets of ground motions were selected. Then, IDA was performed in sequence using the mainshock and aftershock records. The fragility curves were finally computed from the analysis results. Meanwhile, other authors such as Ibrahim and El-Shami (2011) and Shome et al. (2014) used IDA as an input to develop seismic vulnerability curve.

## 2.5 Performance-Based Seismic Design (PBSD)

Manafpour and Moghaddam (2014) reviewed the advantages and disadvantages of probabilistic PBSD by considering all its constraints and limitations. They found that PBSD provides a quantitative measure for structural damage by considering specific earthquake level.

PBSD can be used for several purposes to:

- (i) obtain better performance results for new buildings,
- (ii) determine performance in accordance with code provisions with the subsequent development of the required adjustment,
- (iii) enhance current provisions to obtain good designs, and
- (iv) provide an efficient retrofit design procedure.

These authors argue that the performance of seismic assessment depends on three factors, namely, the ground motion types, resisting lateral load, and height of the buildings. Meanwhile, PBSD can be determined based on the percentage of maximum interstorey drift. Interstorey drift was used because this factor can be easily measured during the analysis and provides a clear result. Interstorey drift can be classified into five categories, namely, operational phase (OP), immediate occupancy (IO), damage control (DC), life safety (LS), and collapse prevention (CP) (Ibrahim and El-Shami 2011). By contrast, other authors, such as Uma et al. (2011), classified interstorey drift into slight, moderate, extensive, complete, and collapse. Table 2.6 summarizes each limit state with the percentage of maximum drift.

**Table 2.6** Summary of performance level and percentage of maximum drift

| Authors                                  | Performance level (%) |       |        |        |        |
|--|-----------------------|-------|--------|--------|--------|
|  | OP                    | IO    | DC     | LS     | CP     |
| Rosowsky and Ellingwood (2002)           | 0.5                   | 1.0   | –      | <5.0   | >5.0   |
| Lee and Rosowsky (2006)                  | –                     | 1.0   | –      | 2.0    | 3.0    |
| Uma et al. (2011) for New Zealand model  | 0.7                   | 0.14  | 2.0    | 2.6    | 3.9    |
| Uma et al. (2011) for US model           | 0.5                   | 0.14  | 3.0    | 3.5    | 5.3    |
| Ibrahim and El-Shami (2011)              | 0.5                   | 1.0   | 1.5    | 2.0    | 2.5    |
| Ruiz-García and Negrete-Manriquez (2011) | –                     | 0.7   | –      | 2.5    | 5.0    |
| Li et al. (2014)                         | –                     | 0.7   | –      | 2.5    | 5.0    |
| Silva et al. (2014)                      | 0.05                  | 0.3   | 1.15   | 2.8    | >4.36  |
| Shin et al. (2014)                       | –                     | 1.0   | 2.0    | 4.0    | >4.0   |
| Aiswarya and Mohan (2014)                | –                     | 1.0   | –      | 2.0    | 4.0    |
| Negulescu et al. (2014)                  | 0.0031                | 0.004 | 0.0066 | 0.0119 | 0.0207 |
| Pragalath et al. (2015)                  | –                     | 1.0   | –      | 2.0    | 4.0    |

Ibrahim and El-Shami (2011) defined each limit state. The building is at an OP state when it is suitable for normal use with least or no damage. At an IO state, the building has minimal or no structural damage and minor non-structural damage. The LS state is when the building appears to have structural and non-structural damages, which require repairs before re-occupancy. At a CP state, the structural and non-structural parts of the building are prevented from collapsing. Meanwhile, Silva et al. (2014) define drift as slightly damaged when 50% of maximum base shear capacity is achieved. The drift is in a moderate state when 75% of maximum base shear capacity is achieved and is in a collapsed state when the ultimate drift taken from the pushover curve is decreased by 20 or 75% (whichever comes first).

A few guidelines, such as FEMA-356 and ATC-40, have been established to improve building performance (Charalambos et al. 2014). The PEER center methodology has been proposed to gain an overall assessment of building performance at any intensity level and limit state by integrating data related to seismic hazard and damage from the structural analysis and loss.

## 2.6 Methods to Develop Fragility Curves

The fragility curves are an important tool to assess seismic risk. Every building or structure has its own fragility curve. This seismic fragility curves can be used as follows:

- (i) for assessing potential effects and risks, including functional and loss in economic and lives,
- (ii) for emergency or disaster response planning, and
- (iii) for risk mitigation efforts (retrofitting).

Based on the literature review, four methods to develop fragility curves can be identified, namely: (i) expert-based or judgmental, (ii) empirical, (iii) analytical, and (iv) hybrid. Billah and Alam (2014) present the advantages and disadvantages of each method to develop fragility curves (Table 2.7).

Figure 2.2 shows the flowchart of the commonly used methodologies to develop fragility curve. Among these methods, analytical fragility curves are the most widely used (Lee and Moon 2014). All of these methods will be explained in detail in the subsequent sections.

### 2.6.1 Expert-Based Method

Expert-based method or heuristic method is the oldest and simplest one among those mentioned above. Here, the damage distribution of a building subjected to

**Table 2.7** Advantages and disadvantages of each method (Billah and Alam 2014)

| Method       | Advantages   | Disadvantages   |
|--------------|--|---|
| Expert based | Simple method<br>All factors may be included                         | Very subjective<br>Totally dependent on the panel expertise<br>Not so accurate                                    |
| Empirical    | Show the actual vulnerability<br>Represent a realistic picture       | Lack of data<br>Inconsistency in damage observation   |
| Analytical   | Less biased<br>All types of uncertainties are considering            | Costly computation<br>Takes too long  |
| Hybrid       | Consider post-earthquake data<br>Computational effort can be reduced | Require multiple data because of combination of experimental and analytical<br>High inconsistency in demand model |

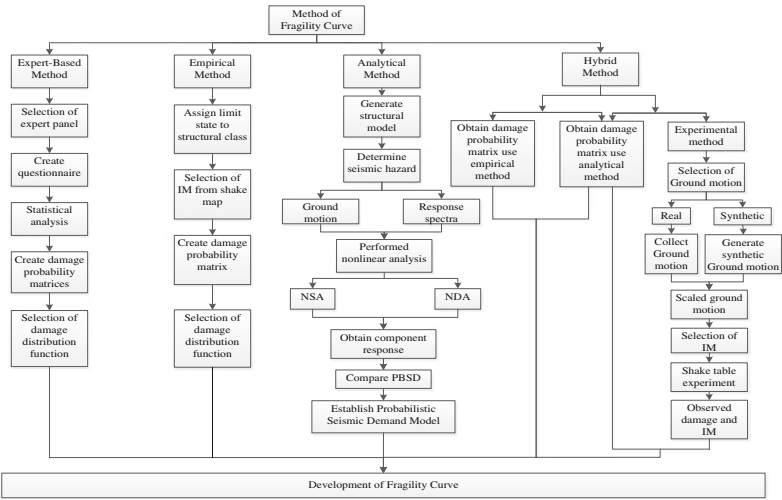


**Fig. 2.2** Methods and steps to develop the fragility curve

different earthquake intensities is estimated by civil engineers, who are deemed experts in the field of earthquake engineering.

Fragility estimates are found from the probability distribution of the damage state at each intensity level. ATC-13 and ATC-40 reports have been specifically prescribed for methods based on expert opinions (Farsangi et al. 2014).

Billah and Alam (2014) added information about ATC-13; in their report, the damage matrices and risks for typical infrastructures in California were documented by 42 expert opinions. In accordance with their responses, the probability damage matrix was developed based on the modified Mercalli intensity value. Expert

opinion is the only source for this method. Thus, this method depends on the use of questionnaires, the experiences of experts, and the number of experts consulted. In general, their judgments or opinions may contain uncertainties and may be less accurate, thus affecting the quality of the result.

### 2.6.2 Empirical Method

The fragility curve developed by this empirical method is based on previous earthquake events. For example, the fragility curves were developed using damage data from the 1995 Kobe earthquake. The curves were established by assuming the measurement error; the intensity measure is insignificant.

Ioannou et al. (2015) used this approach to generate seismic curves for a reinforced concrete frame. The whole process is clearly explained in their paper. They initially determined the seismic damage by modeling two uncertainties, after which they simulated ground motions. Finally, they used Eq. (2.1) to generate the fragility curves based on the empirical method. The resulting equation is given by Eqs. (2.3) and (2.4).

$$Y_{jk} | \text{IM}_{\text{true}} = \text{iml}_{\text{true}.k} \sim \left( \frac{n}{y_{jk}} \right) \mu_{jk}^{y_{jk}} [1 - \mu_{jk}]^{n-y_{jk}} \quad (2.3)$$

where,

$$\mu_{jk} = P(\text{DS} \geq \text{ds}_i | \text{iml}_{\text{true}.k}) = \Phi \left( \frac{\ln(\text{iml}_{\text{true}.k}) - \lambda_k}{\zeta_k} \right) \quad (2.4)$$

$\lambda_k$  is the lognormal mean and

$\zeta_k$  is the lognormal standard deviation for realization  $k$  [estimated from Eq. (2.3)].

In conclusion, they argued that variability ground motion may result in flat curves and wide confidence level. A very dense network of ground motion in the recorded data is required to reduce the uncertainty in the empirical fragility curves (Cunha et al. 2014).

### 2.6.3 Analytical Method

The fragility curves can be generated using this technique even if damage data are insufficient. The analytical method is the most popular method in developing vulnerability seismic curves because this approach has less bias. This approach is developed using simulated data from time history analysis of structural model for real or synthetic ground motions (Farsangi et al. 2014).

### 2.6.4 Hybrid Method

Kammula et al. (2014) reported that the weakness of the analytical method is its requirement to produce a realistic model, that is, if the model is improperly designed or unrealistic, then it may result in inaccurate estimation that can affect the fragility curve. Considering this problem, some researchers introduced a hybrid approach to improve the analytical method.

The hybrid fragility curves are derived by combining experimental and analytical methods. According to Kappos et al. (2006), the hybrid approach is a calibrated empirical and analytical method, which is conducted by integrating numerical method to solve a numerical structural model equation. This equation considers the analytical and physical components of a structural system.

By considering both the analytical and physical components, the effect of earthquakes on the structures (e.g., buildings and bridges) can be determined. They showed the step-by-step development of fragility curves for a 6-storey structure with telescoping self-centering energy dissipative bracing systems based on hybrid approach. The establishment of the framework, formulation model, ground motion, and result simulation of the hybrid method was briefly discussed in their paper.

Billah and Alam (2014) reported that the hybrid approach involves large aleatory and epistemic uncertainties, which are important elements in generating a probabilistic curve. According to Cunha et al. (2014), aleatory uncertainties include material properties and wind loads that cannot be reduced by collecting additional information. Meanwhile, epistemic uncertainties include the lack of knowledge and incorrect modeling. However, these uncertainties can be reduced by obtaining more information.

## References

- Aiswarya, S., and N. Mohan. 2014. Vulnerability analysis by the Development of Fragility Curves. *IOSR Journal of Mechanical and Civil Engineering*, 33–40.
- Akhavan, N., Sh. Tavousi Tafreshi, and A. Ghasemi. 2016. Fragility Assessment for vertically Irregular Buildings with Soft Storey. *International Journal of Civil, Environmental, Structural, Construction and Architectural Engineering*, at Barcelona, Spain 10 (10): 1274–1282.
- Akkar, S., H. Sucuoğlu, and A. Yakut. 2005. Displacement-based fragility functions for low-and mid-rise ordinary concrete buildings. *Earthquake Spectra* 21 (4): 901–927. <https://doi.org/10.1193/1.2084232>.
- Alessandri, S., R. Giannini, and F. Paolacci. 2011. A New Method for Probabilistic Aftershock Risk Evaluation of Damaged Bridge. In COMPDYN 2011-III ECCOMAS Thematic Conference on Computational Methods in Structural Dynamics and Earthquake Engineering.
- Ay, B. Ö., and S. Akkar. 2014. Evaluation of a Recently Proposed Record Selection and Scaling Procedure for Low-Rise to Mid-Rise Reinforced Concrete Buildings and Its Use for Probabilistic Risk Assessment Studies. *Earthquake Engineering & Structural Dynamics* 43: 889–908. <https://doi.org/10.1002/eqe.2378>.
- Baker, J.W., T. Lin, and C.B. Haselton. 2014. Ground Motion Selection for Performance-Based Engineering: Effect of Target Spectrum and Conditioning Period. *Performance-based Seismic Engineering: Vision for an Earthquake Resilient Society* 32: 423.



- Bakhshi, A., and P. Asadi. 2013. Probabilistic Evaluation of Seismic Design Parameters of Rc Frames Based on Fragility Curves. *Scientia Iranica* 20: 231–241. <https://doi.org/10.1016/j.scient.2012.11.012>.
- Banihashemi, A.R., and M.H.R. Tavakoli. 2015. Performance-based plastic design method for steel concentric braced frames. *International Journal of Advanced Structural Engineering (IJASE)* 7 (3): 281–293. <https://doi.org/10.1007/s40091-015-0099-0>.
- Barbat, A. H., H. Alejandro, Y.F. Vargas, L.G. Pujades, and J.E. Hurtado. 2012. Probabilistic assessment of the seismic damage in reinforced concrete buildings. A: International symposium computational civil engineering. In Proceedings of the 10th International Symposium Computational Civil Engineering, Iasi, Romania, May 25th, 2012. Iasi, Societatea Academica, 2012, 43–61.
- Billah, A., and M. Alam. 2014. Seismic Fragility Assessment of Highway Bridges: A State-of-the-Art Review. *Structure and Infrastructure Engineering*, 1–29. <https://doi.org/10.1080/15732479.2014.912243>.
- Charalambos, G., V. Dimitrios, and C. Symeon. 2014. Damage Assessment, Cost Estimating, and Scheduling for Post-Earthquake Building Rehabilitation Using BIM. *Computing in Civil and Building Engineering* (2014). ASCE, 398–405. <https://doi.org/10.1061/9780784413616.050#sthash.LO9sx4WX.dpuf>.
- Colapietro, D., A. Netti, A. Fiore, F. Fatiguso, and G.C. Marano. 2014. On the Definition of Seismic Recovery Interventions in Rc Buildings by Non-Linear Static and Incremental Dynamic Analyses. *International Journal of Mechanics* 8: 216–222.
- Cunha, A., E. Caetano, P. Ribeiro, and G. Müller. 2014. Earthquake Risk Analysis of Structures. In 9th International Conference on Structural Dynamic, EURO DYN 2014, Porto, Portugal.
- Cutfield, M., K. Ryan, and Q. Ma. 2016. Comparative life cycle analysis of conventional and base-isolated buildings. *Earthquake Spectra* 32 (1): 323–343.
- Ebrahimian, H., F. Jalayer, D. Asprone, A.M. Lombardi, W. Marzocchi, A. Prota, and G. Manfredi. 2014. A Performance-Based Framework for Adaptive Seismic Aftershock Risk Assessment. *Earthquake Engineering and Structural Dynamics* 43: 2179–2197. <https://doi.org/10.1002/eqe.2444>.
- Farsangi, E.N., F.H. Rezvani, M. Talebi, and S.A. Hashemi. 2014. Seismic Risk Analysis of Steel-MRFs by Means of Fragility Curves in High Seismic Zones. *Advances in Structural Engineering* 17 (9): 1227–1240.
- Frankie, T.M., B. Gencturk, and A.S. Elnashai. 2012. Simulation-based fragility relationships for unreinforced masonry buildings. *Journal of Structural Engineering* 139 (3): 400–410.
- Garcia, H.A. 2014. Modal pushover analysis for seismic vulnerability analysis.
- Goda, K., and M.R. Salami. 2014. Inelastic Seismic Demand Estimation of Wood-Frame Houses Subjected to Mainshock-Aftershock Sequences. *Bulletin of Earthquake Engineering* 12: 855–874. <https://doi.org/10.1007/s10518-013-9534-4>.
- Hancilar, U., E. Çaktı, M. Erdik, G.E. Franco, and G. Deodatis. 2014. Earthquake vulnerability of school buildings: Probabilistic structural fragility analyses. *Soil Dynamics and Earthquake Engineering* 67: 169–178.
- Haselton, C., A. Whittaker, A. Hortaçsu, J. Baker, J. Bray, and D. Grant. 2012. Selecting and scaling earthquake ground motions for performing response-history analyses. Proceedings of the 15th World Conference on Earthquake Engineering.
- HAZUS. 1999. *Earthquake Loss Estimation*. Washington, DC: Technical Manual, National Institute of Building Sciences.
- Holmes, W.T. 1996. Seismic Evaluation of Existing Buildings: State of the Practice. In Proceedings of the 11th World Conference on Earthquake Engineering, Acapulco, Mexico.
- Hwang, H.H., and J.-W. Jaw. 1990. Probabilistic Damage Analysis of Structures. *Journal of Structural Engineering* 116: 1992–2007. [https://doi.org/10.1061/\(ASCE\)0733-9445\(1990\)116:7\(1992\)#sthash.gpYo9OKI.dpuf](https://doi.org/10.1061/(ASCE)0733-9445(1990)116:7(1992)#sthash.gpYo9OKI.dpuf).
- Ibrahim, Y.E., and M.M. El-Shami. 2011. Seismic Fragility Curves for Mid-Rise Reinforced Concrete Frames in Kingdom of Saudi Arabia. *The IES Journal Part A: Civil & Structural Engineering* 4, no. 4: 213–223.

- Ioannou, I., J. Douglas, and T. Rossetto. 2015. Assessing the impact of ground-motion variability and uncertainty on empirical fragility curves. *Soil Dynamics and Earthquake Engineering* 69: 83–92. <https://doi.org/10.1016/j.soildyn.2014.10.024>.
- Jalayer, F., R. De Risi, and G. Manfredi. 2014. Bayesian Cloud Analysis: Efficient Structural Fragility Assessment Using Linear Regression. *Bulletin of Earthquake Engineering*, 1–21. <https://doi.org/10.1007/s10518-014-9692-z>.
- Jeon, J., R. DesRoches, I. Brilakis, and L. Lowes. 2012. Aftershock fragility curves for damaged non-ductile reinforced concrete buildings. In 15th World Conf. on Earthquake Engineering, International Association for Earthquake Engineering (IAEE), Tokyo, Japan.
- Joy, R., C.K. Prasad, and V. Thampan. 2016. Development of Analytical Fragility Curve—A Review, 713–716.
- Kammula, V., J. Erochko, O.S. Kwon, and C. Christopoulos. 2014. Application of Hybrid-Simulation to Fragility Assessment of the Telescoping Self-Centering Energy Dissipative Bracing System. *Earthquake Engineering and Structural Dynamics* 43: 811–830. <https://doi.org/10.1002/eqe.2374>.
- Kappos, A.J., G. Panagopoulos, C. Panagiotopoulos, and G. Penelis. 2006. A Hybrid Method for the Vulnerability Assessment of R/C and Urm Buildings. *Bulletin of Earthquake Engineering* 4: 391–413. <https://doi.org/10.1007/s10518-006-9023-0>.
- Kircher, C. A., A.A. Nassar, O. Kustu, and W.T. Holmes. 1997. Development of Building Damage Functions for Earthquake Loss Estimation. *Earthquake Spectra* 13: 663–682. <https://doi.org/10.1193/1.1585974>.
- Kirçil, M.S., and Z. Polat. 2006. Fragility Analysis of Mid-Rise R/C Frame Buildings. *Engineering Structures* 28: 1335–1345. <https://doi.org/10.1016/j.engstruct.2006.01.004>.
- Kiremidjian, A.S. 1992. Methods for Regional Damage Estimation. In Proceedings of the 10th World's Conference on Earthquake Engineering, Madrid, Spain, 19–24.
- Kumar, C.R., K.B. Narayan, and D.V. Reddy. 2014. Probabilistic Seismic Risk Evaluation Of RC Buildings. *International Journal of Research in Engineering and Technology* 03 (01): 484–495.
- Kumitani, S., and T. Takada. 2004. Probabilistic Assessment of Buildings Damage Considering Aftershocks of Earthquakes. In 13th World Conference on Earthquake Engineering, Vancouver, BC, Canada.
- Lee, Y., and D. Moon. 2014. A new methodology of the development of seismic fragility curves. *Smart Structures and Systems* 14 (5): 847–867.
- Lee, J., S. Han, and J. Kim. 2014. Seismic Performance Evaluation of Apartment Buildings with Central Core. *International Journal of High-Rise Buildings* 3 (1): 9–19.
- Lee, K.H., and D.V. Rosowsky. 2006. Fragility Analysis of Woodframe Buildings Considering Combined Snow and Earthquake Loading. *Structural Safety* 28: 289–303. <https://doi.org/10.1016/j.strusafe.2005.08.002>.
- Li, Y., R. Song, and J.W. Van De Lindt. 2014. Collapse Fragility of Steel Structures Subjected to Earthquake Mainshock-Aftershock Sequences. *Journal of Structural Engineering*.
- Lin, K., Y. Li, X. Lu, and H. Guan. 2017. Effects of seismic and progressive collapse designs on the vulnerability of RC frame structures. *Journal of Performance of Constructed Facilities* 31 (1): 04016079.
- Luco, N., and C.A. Cornell. 1998. Effects of random connection fractures on the demands and reliability for a 3-story pre-Northridge SMRF structure. In Proceedings of the 6th US national conference on earthquake engineering, vol. 244, 1–12.
- Luco, N., M. Gerstenberger, S. Uma, H. Ryu, A. Liel, and M. Raghunandan. 2011. A Methodology for Post-Mainshock Probabilistic Assessment of Building Collapse Risk. In Ninth Pacific Conference on Earthquake Engineering, Auckland, New Zealand.
- Lupoi, G., P. Franchin, A. Lupoi, and P.E. Pinto. 2006. Seismic Fragility Analysis of Structural Systems. *Journal of Engineering Mechanics* 132: 385–395. [https://doi.org/10.1061/\(ASCE\)0733-9399\(2006\)132:4\(385\)#sthash.NktwK9pH.dpuf](https://doi.org/10.1061/(ASCE)0733-9399(2006)132:4(385)#sthash.NktwK9pH.dpuf).

- Manafpour, A.R., and P.K. Moghaddam. 2014. Probabilistic Approach to Performance-Based Seismic Design of RC Frames. Vulnerability, Uncertainty, and Risk: Quantification, Mitigation, and Management, ASCE, 1736–1745.
- McCrum, D.P., G. Amato, and R. Suhail. 2016. Development of Seismic Fragility Functions for a Moment Resisting 44: 42–51. <https://doi.org/10.2174/1874836801610010042>.
- Modica, A., and P.J. Stafford. 2014. Vector Fragility Surfaces for Reinforced Concrete Frames in Europe. *Bulletin of Earthquake Engineering*, 1–29. <https://doi.org/10.1007/s10518-013-9571-z>.
- Mosalam, K. M., G. Ayala, R.N. White, and C. Roth. 1997. Seismic Fragility of Lrc Frames with and without Masonry Infill Walls. *Journal of Earthquake Engineering* 1: 693–720. <https://doi.org/10.1080/13632469708962384>.
- Nazri, F., and N. Alexander. 2012. Predicting the Collapse Potential of Structures in Earthquake. University of Bristol.
- Negulescu, C., T. Ulrich, A. Baills, and D. Seyedi. 2014. Fragility Curves for Masonry Structures Submitted to Permanent Ground Displacements and Earthquakes. *Natural Hazards*, 1–14. <https://doi.org/10.1007/s11069-014-1253-x>.
- Pejovic, J., and S. Jankovic, 2016. Seismic fragility assessment for reinforced concrete high-rise buildings in Southern Euro-Mediterranean zone. *Bulletin of Earthquake Engineering* 14 (1): 185–212.
- Polese, M., M. Di Ludovico, A. Prota, and G. Manfredi. 2013. Damage-Dependent Vulnerability Curves for Existing Buildings. *Earthquake Engineering and Structural Dynamics* 42: 853–870. <https://doi.org/10.1002/eqe.2249>.
- Polese, M., M. Marcolini, G. Zuccaro, F. Cacace. 2014. Mechanism based assessment of damage-dependent fragility curves for RC building classes. *Bulletin of Earthquake Engineering*, 1–23. <https://doi.org/10.1007/s10518-014-9663-4>.
- Pragalath, D.H., R. Davis, and P. Sarkar. 2015. Reliability Evaluation of Rc Frame by Two Major Fragility Analysis Methods. *Asian Journal of Civil Engineering (BHRC)* 16: 47–66.
- Raghunandan, M., A.B. Liel, and N. Luco. 2014. Aftershock collapse vulnerability assessment of reinforced concrete frame structures. *Earthquake Engineering & Structural Dynamics*. <https://doi.org/10.1002/eqe.2478>.
- Reasenber, A.P., and M.L. John. 2005. Some Facts About Aftershocks to Large Earthquakes in California. USGS open file report, 96–266.
- Réveillère, A., P. Gehl, D. Seyedi, and H. Modaressi. 2012. Development of Seismic Fragility Curves for Mainshock-Damaged Reinforced-Concrete Structures. In Proceedings of the 15th World Conference on Earthquake Engineering.
- Rosowsky, D.V., and B.R. Ellingwood. 2002. Performance-based engineering of wood frame housing: Fragility analysis methodology. *Journal of Structural Engineering* 128 (1): 32–38.
- Ruiz-García, J., and J.C. Negrete-Manriquez. 2011. Evaluation of Drift Demands in Existing Steel Frames under as-Recorded Far-Field and near-Fault Mainshock–Aftershock Seismic Sequences. *Engineering Structures* 33: 621–634. <https://doi.org/10.1016/j.engstruct.2010.11.021>.
- Ryu, H., N. Luco, S. Uma, and A. Liel. 2011. Developing Fragilities for Mainshock-Damaged Structures through Incremental Dynamic Analysis. In Ninth Pacific Conference on Earthquake Engineering, Auckland, New Zealand.
- Seya, H., M.E. Talbott, and H.H. Hwang. 1993. Probabilistic Seismic Analysis of a Steel Frame Structure. *Probabilistic Engineering Mechanics* 8: 127–136. [https://doi.org/10.1016/0266-8920\(93\)90006-H](https://doi.org/10.1016/0266-8920(93)90006-H).
- Shin, J., J. Kim, and K. Lee. 2014. Seismic Assessment of Damaged Piloti-Type Rc Building Subjected to Successive Earthquakes. *Earthquake Engineering and Structural Dynamics*. <https://doi.org/10.1002/eqe.2412>.
- Shinozuka, M., M.Q. Feng, H.-K. Kim, and S.-H. Kim. 2000. Nonlinear static procedure for fragility curve development. *Journal of Engineering Mechanics* 126 (12): 1287–1295.

- Shome, N., N. Luco, M.C. Gerstenberger, O.S. Boyd, N.E.H. Field, A.B. Liel, and J.W. van de Lindt. 2014. Aftershock Risks Such as Those Demonstrated by the Recent Events in New Zealand and Japan.
- Silva, V., H. Crowley, H. Varum, R. Pinho, and L. Sousa. 2014a. Development of a Fragility Model for Moment-frame RC buildings in Portugal. 2nd ICVRAM, Liverpool, UK.
- Silva, V., H. Crowley, H. Varum, R. Pinho, and R. Sousa. 2014b. Evaluation of Analytical Methodologies Used to Derive Vulnerability Functions. *Earthquake Engineering and Structural Dynamics* 43: 181–204. <https://doi.org/10.1002/eqe.2337>.
- Singhal, A., and A.S. Kiremidjian. 1996. Method for Probabilistic Evaluation of Seismic Structural Damage. *Journal of Structural Engineering-ASCE* 122: 1459–1467. [https://doi.org/10.1061/\(ASCE\)0733-9445\(1996\)122:12\(1459\)#sthash.0ACtmOb5.dpuf](https://doi.org/10.1061/(ASCE)0733-9445(1996)122:12(1459)#sthash.0ACtmOb5.dpuf).
- Siqueira, G.H., A.S. Sanda, P. Paultre, and J.E. Padgett. 2014. Fragility Curves for Isolated Bridges in Eastern Canada Using Experimental Results. *Engineering Structures* 74: 311–324. <https://doi.org/10.1016/j.engstruct.2014.04.053>.
- Song, R., Y. Li, and J.W. van de Lindt. 2014. Impact of Earthquake Ground Motion Characteristics on Collapse Risk of Post-Mainshock Buildings Considering Aftershocks. *Engineering Structures* 81: 349–361. <https://doi.org/10.1016/j.engstruct.2014.09.047>.
- Sudret, B., C. Mai, and V. Mai. 2013. Computing seismic fragility curves using polynomial chaos expansions, Eidgenössische Technische Hochschule Zürich.
- Sudret, B., C. Mai, and K. Konakli. 2014. Computing seismic fragility curves using non-parametric representations. [arXiv:1403.5481](https://arxiv.org/abs/1403.5481).
- Uhrhammer, R.A. 1986. Characteristics of Northern and Central California Sesimicity. *Earthquake Notes* 21.
- Uma, S., H. Ryu, N. Luco, A. Liel, and M. Raghunandan. 2011. Comparison of Main-Shock and Aftershock Fragility Curves Developed for New Zealand and Us Buildings. In Proceedings of the ninth pacific conference on earthquake engineering structure building and Earthquake-Resilient Society, Auckland, New Zealand, 14–16.
- Vargas, Y.F., L.G. Pujades, A.H. Barbat, and J.E. Hurtado. 2013. Capacity, Fragility and Damage in Reinforced Concrete Buildings: A Probabilistic Approach. *Bulletin of Earthquake Engineering* 11: 2007–2032. <https://doi.org/10.1007/s10518-013-9468-x>.
- Vona, M. 2014. Fragility Curves of Existing Rc Buildings Based on Specific Structural Performance Levels. *Open Journal of Civil Engineering*. <https://doi.org/10.4236/ojce.2014.42011>.
- Wang, Y., and D.V. Rosowsky. 2014. Effects of Earthquake Ground Motion Selection and Scaling Method on Performance-Based Engineering of Wood-Frame Structures. *Journal of Structural Engineering*. [https://doi.org/10.1061/\(ASCE\)ST.1943-541X.0001016#sthash.RitmuRN9.dpuf](https://doi.org/10.1061/(ASCE)ST.1943-541X.0001016#sthash.RitmuRN9.dpuf).
- Wells, L.A., and K.J. Coppersmith. 1994. New empirical relationships among magnitude, rupture length, rupture width, rupture area and surface displacement. *Bulletin of the Seismological Society of America* 84 (4): 974–1002.
- Wijayanti E., F. Kristiawan, E. Purwanto, and S. Sangadji. 2016. Seismic vulnerability of reinforced concrete building based on the development of fragility curve: A case study. *Applied Mechanics and Materials* 845: 252–258. doi:[10.4028/www.scientific.net/AMM.845.252](https://doi.org/10.4028/www.scientific.net/AMM.845.252)
- Yamaguchi, N., and F. Yamazaki. 2000. Fragility curves for buildings in Japan based on damage surveys after the 1995 Kobe earthquake. In Proceedings of the 12th conference on earthquake engineering, Auckland, New Zealand.

Seismic Fragility Assessment for Buildings due to  
Earthquake Excitation

NAZRI, F.M.

2018, VIII, 114 p. 38 illus., 32 illus. in color., Softcover

ISBN: 978-981-10-7124-9